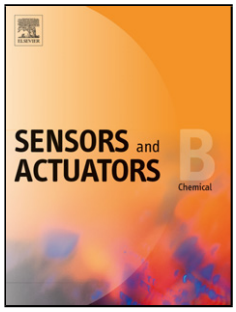

Title: Facile synthesis of carbon nanoparticles from sodium alginate via ultrasonic-assisted nano-precipitation and thermal acid dehydration for ferric ion sensing

Author: Jessica Fung Yee Fong Suk Fun Chin Sing Muk Ng

PII: S0925-4005(14)01583-4
DOI: http://dx.doi.org/doi:10.1016/j.snb.2014.12.038
Reference: SNB 17828

To appear in: *Sensors and Actuators B*

Received date: 30-7-2014
Revised date: 6-12-2014
Accepted date: 9-12-2014

Please cite this article as: J.F.Y. Fong, S.F. Chin, S.M. Ng, Facile synthesis of carbon nanoparticles from sodium alginate via ultrasonic-assisted nano-precipitation and thermal acid dehydration for ferric ion sensing, *Sensors and Actuators B: Chemical* (2014), http://dx.doi.org/10.1016/j.snb.2014.12.038

Sensors & Actuators B (Full paper)

Facile synthesis of carbon nanoparticles from sodium alginate via ultrasonic-assisted nano-precipitation and thermal acid dehydration for ferric ion sensing

Jessica Fung Yee Fong [a,b], Suk Fun Chin [c], Sing Muk Ng [a, b]*

[a] Faculty of Engineering, Computing and Science, Swinburne University of Technology Sarawak Campus, Jalan Simpang Tiga, 93350 Kuching, Sarawak, Malaysia.

[b] Swinburne Sarawak Research Centre for Sustainable Technologies, Swinburne University of Technology Sarawak Campus, Jalan Simpang Tiga, 93350 Kuching, Sarawak, Malaysia.

[c] Faculty of Resource Science and Technology, Universiti Malaysia Sarawak, 94300 Kota Samarahan, Sarawak, Malaysia.

* Corresponding author at: Tel: +6082-260848 Fax: +6082-260813
Email address: smng@swinburne.edu.my

Abstract

Carbon nanoparticles have emerged as a promising alternative to the well-known quantum dots in many biological applications due to their excellent optical properties and biocompatibility. It has received considerable attentions from researchers especially in the aspects of producing these carbon nanomaterials via easier and cheaper synthetic routes. On this motivation, we hereby report an economical and facile synthesis of carbon nanoparticles from alginate via a simple two-step procedure; nano-precipitation through ultrasonication followed by thermal acid carbonisation. Nano-precipitation was first performed on the alginate stock solution to produce nanoparticles with controlled morphology. Precipitation was performed in acidic solution that has coagulated the alginate chains into nanoparticles. Ultrasonic treatment was found crucial to assist the formation of nanoparticles that were more homogenous in the size distribution at around 100 nm. The shape was also more spherical as compared to those without ultrasonic treatment. In the carbonisation step, thermal dehydration was employed using concentrated sulphuric acid that has successfully converted the preformed alginate nanoparticles into carbon nanoparticles. The carbon nanoparticles isolated showed high fluorescence even without further surface passivation. The fluorescence of these carbon nanoparticles were utilised for sensitive and selective sensing of ferric ions and it was evaluated to have a linear analytical dynamic range up to 25 μM with a limit of detection (LOD) as low as 1.06 μM. The system was successfully employed to detect ferric ions in real water sample.

Keywords

- Carbon nanoparticles
- Nano-precipitation

- Carbonisation
- Photoluminescence properties
- Optical sensing

1. Introduction

In the past decades, quantum dots (QDs) that are highly fluorescent have attracted considerably intense research interests as to understand the basic physicochemical properties to utilise them for different applications. For instance, the tuneable photoluminescence property has earned QDs a reputable use in the biomedical field such as for bio-imaging and sensing [1]. Although QDs show great flexibility in their tuneable and bright photoluminescence, the *in vivo* toxicity remains a major concern as QDs consist of heavy metal precursors such as cadmium and selenium. The leaching of these heavy metals from QDs during the application stage will be harmful, both to human body and the environment [2]. Therefore, alternative fluorescent materials that can demonstrate comparable optical properties to the QDs, but possess low or no toxicity risk are in need to replace the use of QDs.

Recently, carbon nanoparticles (CNPs) or commonly known as carbon dots were discovered to show excellent fluorescence properties. This has raised a substantial amount of attention to replace the use of QDs with CNPs for various applications. CNPs which are comprised of carbon as its primary constituent, likewise to the other nano-forms such as fullerene, nanodiamond, carbon nanotubes and graphene often show low or no toxicity effect. In addition, CNPs are highly biocompatible, produce non-blinking fluorescence, economical to produce, and easy to synthesise [2, 3]. Due to these unique properties, CNPs have been classified as a new class of its own within the carbon nanomaterial group, referred as the *quasi*spherical dots with sizes in the nanometres range. Similar to QDs, this group exhibits tuneable fluorescence emission with distinguishable Stoke shift that can be an important criterion for some applications such as optical sensing. In view of that, CNPs have rapidly

emerged to become one of the promising alternatives for bio-imaging, smart sensing, specific metal ion sensing, optoelectronics, drug delivery, etc. [2, 4].

CNPs were first discovered serendipitously in an event of electrophoretic purification of single-walled carbon nantubes (SWCNTs) synthesised from arc-discharge soot [5]. Since then, many have looked into different routes to produce high quality CNPs which are generally categorised in two approaches; top-down and bottom-up. The top-down approach takes place when CNPs are formed from a larger structure such as bulk graphite. It usually involves complicated instrumental setups, expensive precursors, or complicated processes. Some examples include the use of laser ablation [6, 7], laser irradiation of graphite flakes [8], and electrochemical treatment of CNPs [9]. On the other hand, the bottom-up approach produces CNPs from molecular precursors via various methods such as hydrothermal treatment [10, 11], pyrolysis [12] and microwave-assisted carbonization [13]. In many aspects, bottom-up approach is better compared to the top-down approach. For instance, Peng and Travas-Sejdic [14] have first demonstrated a simple aqueous solution route to obtain luminescent CNPs from carbohydrates such as starch, glucose and sucrose. They have converted the starting precursors using acid dehydration approach and further passivated the surface of the CNPs using nitric acid for 12 hours. Nonetheless, the approach sometimes has several drawbacks, including multiple steps procedure and prolonged hours of reaction.

We herein report a facile synthesis of CNPs from alginate precursor, which is a negatively charged polysaccharide of algal origins [15]. Alginate was selected as the molecular precursor for the synthesis as it is a U.S. Food and Drug Administration (FDA) approved food additive and is certified to be safe for human consumption [16]. Alginate has also been used widely in the biomedical applications including drug delivery that showed good biocompatibility. This minimises possible toxicity issues for the produced CNPs and can potentially be adopted for biomedical applications in future at a higher confidence level. To

the best of our knowledge till date, there is no report yet on the production of CNPs from alginate nanoparticles that were pre-formed via ultrasonic-assisted nano-precipitation of alginate in acidic solvent. The aforementioned step was first carried out to produce precursors with smaller particle size and therefore can increase the carbonisation efficiency due to higher total surface area. These nanoparticles were then used as molecular precursor for the subsequent thermal acid dehydration process to synthesize the fluorescent CNPs without the need of further surface passivation. The work will demonstrate a novel approach to synthesise CNPs with high efficiency at a much reduced reaction time. Furthermore, the acid hydrolysis process has given rise to the carboxyl and hydroxyl groups on the surface of the CNPs. This will be ideal to be used for ions sensing application as demonstrated later in this work.

2. Experimental

2.1. Reagents/Materials

Sodium alginate was purchased from Sigma Aldrich (USA). Sulfuric acid (H_2SO_4), sodium hydroxide (NaOH), ethyl acetate (EtoAc), sodium nitrate ($NaNO_3$), potassium nitrate (KNO_3), calcium chloride ($CaCl_2$), barium chloride ($BaCl_2$), manganese chloride ($MnCl_2$), lead nitrate ($Pb(NO_3)_2$), cobalt nitrate ($Co(NO_3)_2$), nickel nitrate ($Ni(NO_3)_2$), copper nitrate ($Cu(NO_3)_2$), silver nitrate ($AgNO_3$), chromium nitrate ($Cr(NO_3)_3$), zinc nitrate ($Zn(NO_3)_2$), iron nitrate ($Fe(NO_3)_3$), mercury chloride ($HgCl_2$), magnesium nitrate ($Mg(NO_3)_2$), tin chloride ($SnCl_2$) were purchased from R&M Marketing (Malaysia) and Merck (Germany). The chemicals were of analytical grade unless otherwise stated and used as received without further purification. Ultrapure water used throughout the experiments was obtained from Mili-Q milipore system (18.2 MΩ).

116 2.2. Instrumentation

117 All fluorescence measurements were carried out using a fluorescence spectrophotometer
118 (Cary Eclipse, Varian) under fluorescence mode with both excitation and emission slits set at
119 10 nm. The sample was diluted in ultrapure water in an appropriate volume for fluorescence
120 analysis, placed in a quartz cuvette with path length of 1.0 cm. The absorption measurements
121 were carried out using UV-Vis spectrophotometer (Cary® 50 UV-Vis, Varian). Morphology
122 and size of alginate nanoparticles were observed using a Scanning Electron Microscope
123 (SEM) operated at 10kV (JEOL JSM-6930 LA) while morphology of CNPs was observed
124 under a Transmission Electron Microscope (TEM) at 80 kV (JEOL-2000) on the copper grid.
125 Fourier transformed infrared (FTIR) spectra were obtained using a FTIR spectroscope
126 (Nicolet iS10, PerkinElmer).

127 2.3. Preparation of CNPs

128 The synthesis approach performed in this study was in reference to previous work reported
129 with necessary modifications [17]. In the typical synthesis, 2.0 mL of alginate solution (0.1
130 w/v %) was added dropwise into 5.0 mL of sulphuric acid (0.1 M), which acted as a non-
131 solvent to form the precipitate. The system was left sonicating for 1 hour to form the
132 nanoparticles. As for comparison, same initial steps were repeated on a separate set but by
133 stirring using a magnetic stirrer for 1 hour instead of using an ultrasonicator. Next, 6.0 mL of
134 concentrated sulphuric acid (~18 M) was added carefully into the mixture and followed by
135 transferring the sample into a drying oven that was pre-set with a consistent heating
136 temperature of 120 °C. The carbonisation process was left for 4 hours in the oven. Another
137 set of the CNPs preparation was carried out in room temperature setting (~25°C). Next, the
138 crude product obtained was neutralised using 20.0 mL of NaOH (~10 M) and the CNPs were
139 extracted from the residue using 60.0 mL of ethyl acetate via pH-dependent approach.
140 Following that, anhydrous magnesium sulphate was added to the ethyl acetate and later

141 filtered off. The solvent was removed under vacuum to collect the CNPs and were re-
142 dispersed in ultrapure water for further characterisations.

143 2.4. Quantum yield measurement

144 Quinine sulfate in 0.1 M H_2SO_4 (QY=0.54 at excitation wavelength of 350 nm) was selected
145 as the standard for quantum yield (QY) measurement using a comparative method. The
146 concentration of the sample was adjusted to obtain absorbance below 0.1 in order to
147 minimize the inner filter effect. The QY of CNPs was determined according to the following
148 equation:

149 $$QY = QY_R \frac{I}{I_R}\frac{A_R}{A}\frac{n^2}{n_R^2}$$

150 where *I* denotes the integrated fluorescence intensity, *A* is the absorbance value and *n* as the
151 refractive index.

152 2.5. Fluorescent sensing of Fe(III) ions

153 Stock solution of Fe(III) ions (0.1M) was prepared from its salt and subsequent dilutions
154 were performed using this stock for further analytical studies. To investigate the sensing
155 potential of the CNPs towards Fe(III) ions, 100 μL of the synthesised CNPs were diluted in
156 3.0 mL of ultrapure water and the fluorescence signal was monitored at the wavelength of
157 440 nm. The recorded intensity was taken as baseline signal. Following this, Fe(III) ions
158 solution was titrated stepwise into this solution and the corresponding fluorescence intensities
159 at the same wavelength after each addition were recorded respectively. Sensing signal was
160 taken as the change in the intensity compared to the baseline signal after the addition of Fe(III)
161 ions.

2.6. Cations selectivity analysis

Stock solutions (0.1M) for various metal ions were prepared from the respective salts and used to investigate the possible interfering effect on the proposed sensing system. Particularly for this study, Na(I), K(I), Mg(II), Ca(II), Ba(II), Cr(III), Mn(II), Fe(III), Co(II), Ni(II), Cu(II), Ag(I), Zn(II), Hg(II), Sn(II), Pb(II) ions were chosen since these ions co-exist commonly with Fe(III) ions in nature. To perform the test, 100 μL of the synthesised CNPs was diluted with 3.0 mL of milipore water. To this solution, the respective metal ions solutions were added twice at an interval of 25 μL and the change in the intensity before and after the addition was recorded for each interval. In order to study the efficiency of Fe(III) ions sensing in the presence of the possible interfering ions, Fe(III) ions was added with the respective interference ions at a molar ratio of 1:1 and tested similarly for the CNPs response. The concentrations for Fe(III) ions and interfering ions were fixed at 1.56 mM respectively.

3. Results and Discussion

3.1. Preparation of CNPs

3.1.1. Ultrasonic-assisted nano-precipitation

The first step of the synthesis method carried out was the nano-precipitation of the alginate solution to produce nanoparticles for later use as starting precursor in the CNPs synthesis. The nano-precipitation was found to improve the homogeneity in the morphology of the nanoparticles, increase the yield efficiency of the fluorescence, and produce nanoparticles of smaller sizes. Ultrasonic treatment is commonly adopted for the synthesis of polymer nanoparticles due to its ability to reduce particle size and to break-up agglomerates without chemical modifications [18, 19]. As observed from the SEM micrographs (Figure 1), the size and morphology of the alginate nanoparticles formed after sonication process was

significantly different from the batch produced by magnetic stirring. The shape was more homogenous with an average size at around 100 nm.

3.1.2. Thermal-assisted acid dehydration

CNPs were produced by carbonising the alginate nanoparticles that were pre-formed using ultrasonic approach without further purification or isolation. The carbonisation process employed concentrated sulphuric acid as strong dehydrating agent. Water molecules will be removed from the carbohydrate chains and subsequently the crosslinking process will occur to form 3D rigid structure of the CNPs. In order to obtain some insights of the carbonisation process, its kinetics was studied by monitoring the yield of the CNPs produced over time. In this case, assumption was made that the net yield produced was directly correlated to the intensity of the fluorescence emission. Such assumption was suggested since CNPs were the only species known to show fluorescence within the mixture, as increment of intensity will imply the increase in yield. When performing the synthesis at room temperature (~25°C), the fluorescence intensity showed a slight increment within the first hour and reached plateau after that (Figure 2a). This implies that prolonged hour will not further promote the formation of CNPs.

Alternative to the common room temperature acid dehydration [14], higher carbonisation temperature set at 120°C was investigated. Heating was found to have improved the carbonisation process as indicated by the significant enhancement in the fluorescence intensity recorded over time (Figure 2b). CNPs produced under higher thermal condition have shown at least 4-folds of increment in fluorescence intensity as compared to those produced at room temperature. High temperature was deduced to provide sufficient activation energy to promote a more complete dehydration reaction during the conversion of alginate nanoparticles into CNPs. The best yield was obtained after 4 hours of heating in the drying

oven. The time taken for the synthesis was comparatively short as compared to some other works that could took up to 12 hours [14].

3.1.3. Extraction of CNPs

CNPs in this study were extracted from the crude carbon residues collected after the acid dehydration process. Ethyl acetate was employed for the extraction based on the pH-dependent partitioning nature of the CNPs in two different solvents. As the CNPs isolated were produced via acid carbonisation, it can act as weak acid due to the presence of carboxyl groups on the surface of CNPs. Thus by controlling the pH condition, the solubility of the CNPs in a solvent can be altered easily, allowing pH-dependent extraction to be carried out. More effective extraction was achieved by maintaining the pH at a lower value of the crude residues during the extraction. Under this condition, CNPs were protonated and will promote better solubility in ethyl acetate as compared to aqueous media. The CNPs isolated from this extraction approach were purer and low or free from ionic salts, which were produced as side products during the carbonisation process. Dialysis could be another purification option to be adopted especially for the removal of ionic salts, but the process is often lengthy and the progress is difficult to monitor. After the extraction, ethyl acetate was removed using vacuum concentrator and the CNPs were dispersed in water for further use.

3.2. Characterisation

3.2.1. Morphology

The size and morphology of the CNPs isolated were observed under a TEM. In general, the synthesis approach performed has managed to produce CNPs that were highly homogenous in shape and size. Instead of the common *quasi*spherical shape, CNPs obtained in this study were slightly oval in shape and within the average size dimensions of 100 nm (Figure 3). The formation of such morphology could be due to the two-step synthesis approach taken to produce the CNPs. At the stage where the alginate nanoparticles were first produced, the

234 tendency of agglomeration was high due to the high surface energy. Interaction can occur
235 between the nanoparticles, causing distortion of the sphere dimension of the polymeric
236 droplets. However, effective physical contact to form larger clusters was not possible due to
237 the ultrasonic energy applied during the precipitation process. This was strongly supported by
238 the evidence of clusters formation from the sample synthesised without applying ultrasonic
239 treatment as shown in Figure 1(a). At the subsequent carbonisation step, the structure of
240 alginate nanoparticles was frozen up by the cross-linking process induced by the
241 intermolecular dehydration of the alginate polymer chains by the strong acid [20]. Thus, the
242 shape was less spherical, but highly homogeneous in the morphology.

243 *3.2.2. Optical properties*

244 Although the CNPs were not exactly spherical in shape, the optical properties were found
245 similar to the carbon dots reported in the literatures. Figure 4a depicts a typical absorbance,
246 excitation and emission spectrum of CNPs synthesised in this study. The UV-Vis spectra
247 showed a strong absorption in the UV range at the peak of 257 nm which was attributed to
248 the π-π^* transitions. A small shoulder found centring at about 320 nm was caused by the
249 surface defects [21]. The spectrum tail was extending towards the visible range. Fluorescence
250 emissions of the CNPs upon excitation at various wavelengths between 300 and 450 nm were
251 measured. The best fluorescence co-efficient was achieved when the CNPs were excited at
252 340 nm, which produced the emission maximum at a red shift of 100 nm from the excitation
253 wavelength. The fluorescence emissions were consistently peaking at around 440 nm without
254 significant shifting but the intensity decreased at longer excitation wavelengths. This
255 excitation-independent emission was observed upon excitation between 320 nm and 380 nm
256 (Figure 4b). However at excitation above 390 nm, the emission intensity has been
257 significantly decreased and showed a trend of red shift. This showed similarity to a typical
258 photoluminescence feature of carbon dots [22, 23]. This could be due to different energy

levels associated with various "surface states" as a result of different functional groups that contributed to the excitation-dependent emission phenomenon. Similar observation was also obtained by Tang et. al. in their work of synthesising glucose-derived graphene quantum dots [24]. In this study, the excitation-independent emission was observed with excitation wavelengths between 300 and 380 nm, indicating a relatively uniform surface with consistent carboxyl moieties on the CNPs [23]. Using quinine sulphate in H_2SO_4 (0.1 M) as a reference for the photoluminescence QY study, QY of the CNPs obtained in this study was 5.42%, a value that was comparable to most reported QY for CNPs [7, 25].

3.2.3. Mechanism of fluorescence

The origin of fluorescence for CNPs remains unclear but majority works have suggested two most possible explanations; quantum confinement effects due to the nano-sized morphology or band gaps formation due to surface defects of CNPs [2, 26]. Since the average sizes of the CNPs produced in this study were around 100 nm, the fluorescence mechanism due to quantum confinement at these sizes range would be less effective, thus suggesting the more plausible origin as due to the emissive traps on the surface of the CNPs. Furthermore, H_2SO_4 used for the carbonisation process is a good oxidising agent. This leads to the formation of –COOH and –OH groups on the surface of CNPs as shown by the FTIR spectrum (Figure 5b) with the absorption peaks of C=C, C=O and -OH moieties at 1640, 1715 and 3418 cm^{-1} [4]. As a result, these functional groups could form the surface emissive defects and trap photo-induced electrons. The electron-to-hole transitions can occur and subsequently give out fluorescence emission. This suggestion was supported by the observation that alginate nanoparticles heated at 120 °C without the presence of H_2SO_4 showed low or no fluorescence. The obtained FTIR spectrum of the precursor, alginate in Figure 5a showed that the distinctive absorption at 1604 cm^{-1} due to the asymmetric stretching of the carboxylate O-C-O vibration [27] was clearly shifted or changed in that of CNPs (Figure 5b), further affirming

the fact that the chemical structure or conformation of the starting material has changed in the CNPs. The acid dehydration process also resulted in conversion of –OH groups in alginate to C=C bonds in CNPs, indicated by the shifting of absorption peak from 1604 cm^{-1} in alginate to 1640 cm^{-1} in the CNPs. Besides, the absorptions at 2853 and 2923 cm^{-1} attributed to the – CH_2 and CH_3 groups are shown more prominently in CNPs compared to that in alginate. The weak absorption peak at 2361 cm^{-1} due to the acetal groups present in alginate are not observable in FTIR of CNPs. These observations imply the acetal bonds within the long polysaccharide chain have been broken off during the strong acid dehydration process, resulting in the CH_2 and CH_3 groups.

The work by Wang, Cao [28] has reported that the interaction between CNPs and potential electron donor or electron acceptor molecules in close proximity could disrupt the surface emissive sites via energy transfer and consequently causing effective fluorescence quenching. This potential property could be exploited for efficient sensing applications. In addition, CNPs synthesised in this work displayed full width half maximum (FWHM) of 113 nm, which was considerably narrow and implying homogenous distribution on the type of defect formed on the surface. Better homogeneity will be of advantage to generate consistent analytical signals.

3.3. Sensing potential

3.3.1. Sensing of Fe(III) ions

Fe(III) ions have high affinity toward oxygen moiety that is usually rich in electron density. Therefore, the –COOH and –OH formed on the surface of CNPs can act as a good binding sites for the Fe(III) ions, since these groups are rich with oxygen. Fe(III) ions can bind to the sites via coordination bonds to form complex and eventually disrupt the initial electrons transition of the CNPs, promoting quenching once the transition shifted to non-radiation pathways [29]. The disruption of the electronic transition of the CNPs by Fe(III) ions could

be due to the ease of state conversion between different oxidation states. In order to investigate the sensitivity of the CNPs as probe for Fe(III) ions sensing, micro-titration method was performed. The fluorescence of CNPs was found to be quenched accordingly and dependently to the concentration of the Fe(III) ions added to the CNPs (Figure 6). However, the degree of change in the signal intensity at 440 nm corresponding to the concentration of Fe(III) ions was found to be non-linear. In view of this, standard Stern-Volmer quenching relationship as given in the following equation was employed to evaluate the analytical dynamic linear range of the proposed sensing method.

$$F_0/F = 1 + K_{sv}[C]$$

where F_0 and F are each the fluorescence intensities in the absence and presence of Fe(III) ions, K_{sv} being the Stern-Volmer constant and [C] is the concentration of Fe(III) ions.

Using the Stern-Volmer equation, linear relationship between the fluorescence response and the concentration of Fe(III) ions was obtained and found to be $F_0/F = 15791\ [C] + 0.992$, with the correlation coefficient (R^2) of 0.999 (inset Figure 6). Subsequently, the relationship allowed the determination of the limit of detection (LOD) for Fe(III) ions and was evaluated to be 1.06 μM.

Iron is one of the micronutrients essentially used in the biological systems for maintaining good health. The excess of iron in body will however pose a threat to the cells and tissues. Further, overloading of iron in body tissue is often relatable to a number of pathological conditions such as cancer, Alzheimer's disease, liver and kidney disease [31]. Therefore, iron homeostasis is tightly controlled to avoid iron poisoning [32]. Besides that, it is also crucial to monitor iron content in food intake, presence of iron in soil, drinking water, biological samples, and pharmaceuticals. The low detection limit for Fe(III) ions achieved using the

obtained sensing system in this study could therefore be explored and utilised for its potential in Fe(III) ions sensing in water sample.

3.3.2. Selectivity analysis

To investigate the selectivity of the proposed CNPs sensing system, the analytical response of the CNPs towards other metal cations was evaluated. The intensities recorded after each addition is showed in Figure 7. Comparatively, the CNPs were most selective towards the Fe(III) ions within the concentration range tested, where the quenching was almost 80% as compared to the initial signal of blank. Other metal ions have at most only 20% loss within the same concentration range. The reduction of signals that was most likely due to the dilution caused by the increasing volume of water during the micro-titration was also found insignificant and negligible.

The effect of possible interfering cations on Fe(III) ions monitoring was also carried out in the presence of the interfering species rather than individual evaluation. The relative error caused by the interfering ions that present together at a 1:1 ratio was evaluated based on the following equation:

$$\text{Relative error (\%)} = \left| S - S_0 \right| / S_0 \times 100$$

where S_0 and S are the net quenching caused by Fe(III) ions alone and Fe(III) ions in the presence of interfering cations.

Table 1 shows clearly that the interference effect caused by foreign cations tested were not significant where mostly having relative error below 5.0-6.0%, except for Cr(III) and Sn(II). The interference from these two cations might not be too crucial since it is not very abundant in nature. The high selectivity of Fe(III) ions could be due to the sensing mechanism proposed based on the defect on the surface containing oxygen rich groups. Fe(III) ions have comparatively higher positive charge and this allows better attraction to the negative surface

of the CNPs. Besides, Fe(III) ions tend to form stronger interaction with O-donor ligands than with N-donor ligands. Due to this low interference effect by other foreign cations, this proposed method has shown to be robust and feasible to detect Fe(III) ions in multi analytes sample without the need of separation or pre-concentration.

3.3.3. Application to real sample

The potential of sensing Fe(III) ions in real sample was tested using tap water. Iron could be present in the tap water if iron is used as flocculant and due to corrosion of steel from piping system. The allowed concentration of Fe in drinking water according to the European Union (EU) standards is 0.2 mg/L [33]. Since the LOD of our sensing system is as low as 1.06 μM which is translatable as 0.06 mg/L, the Fe(III) ions determination in tap water using the CNPs can be put to practical use. In this study, direct collected samples of tap water showed no significant quenching, indicating low content of Fe(III) ions. In order to demonstrate the practicality of the system for real application, spiked tap water samples were used instead (spiked with known amount of analyte Fe(III) ions, 0-35μM concentration).

The recovery of the Fe(III) ions spiking in tap water is shown in Table 2, with high recovery rate (>94%) and low RSD values. Since proposed for Fe(III) ions detection for water sample, the factor of size for CNPs will not be an issue in comparison with *in-vivo* sensing in the biomedical applications.

4. Conclusions

In summary, we have demonstrated a novel and simple stepwise synthesis of CNPs from alginate; firstly nano-precipitation assisted by ultrasonication and followed by carbonisation using thermal acid dehydration. The ultrasonic treatment during nano-precipitation was proven to produce smaller nanoparticles and subsequently produced CNPs with stronger photoluminescence. The CNPs exhibited strong, stable and non-shifting fluorescence when

excited under long wavelengths. The hydroxyl and carboxyl groups on the surface of the CNPs were able to attract the Fe(III) ions, which allowed the CNPs to be used as sensitive and selective probe for sensing of Fe(III) ions. With the current findings, the proposed sensing probe might be able to be used later for real applications, especially in the biomedical field since the CNPs by nature are less toxic.

Acknowledgement

This work was partially supported by Swinburne Sarawak Research Grant Phase 1/2013 (2-5509) from Swinburne University of Technology Sarawak Campus. Jessica Fong would like to thank Swinburne SUPRA Scholarship for supporting her Ph.D. study.

5. References

[1] L.M. Maestro, J.E. Ramirez-Hernandez, N. Bogdan, J.A. Capobianco, F. Vetrone, J.G. Sole, et al., Deep tissue bio-imaging using two-photon excited CdTe fluorescent quantum dots working within the biological window, Nanoscale, 4(2012) 298-302.

[2] S.N. Baker, G.A. Baker, Luminescent Carbon Nanodots: Emergent Nanolights, Angew Chem Int Ed, 49(2010) 6726-44.

[3] J.C.G. Esteves da Silva, H.M.R. Gonçalves, Analytical and bioanalytical applications of carbon dots, TrAC, Trends Anal Chem, 30(2011) 1327-36.

[4] S. Mohd Yazid, S. Chin, S. Pang, S. Ng, Detection of Sn(II) ions via quenching of the fluorescence of carbon nanodots, Microchim Acta, 180(2013) 137-43.

[5] X. Xu, R. Ray, Y. Gu, H.J. Ploehn, L. Gearheart, K. Raker, et al., Electrophoretic Analysis and Purification of Fluorescent Single-Walled Carbon Nanotube Fragments, J Am Chem Soc, 126(2004) 12736-7.

[6] H. Gonçalves, J.G. Esteves da Silva, Fluorescent Carbon Dots Capped with PEG200 and Mercaptosuccinic Acid, Journal of Fluorescence, 20(2010) 1023-8.

[7] Y.-P. Sun, B. Zhou, Y. Lin, W. Wang, K.A.S. Fernando, P. Pathak, et al., Quantum-Sized Carbon Dots for Bright and Colorful Photoluminescence, Journal of the American Chemical Society, 128(2006) 7756-7.

[8] S. Hu, J. Liu, J. Yang, Y. Wang, S. Cao, Laser synthesis and size tailor of carbon quantum dots, J Nanopart Res, 13(2011) 7247-52.

[9] Z. Kang, H. Ming, Z. Ma, Y. Liu, K. Pan, H. Yu, et al., Large Scale Electrochemical Synthesis of High Quality Carbon Nanodots and Their Photocatalytic Property, Dalton Transactions, 41(2012) 9526-31.

[10] L.Q. Liu, Y.F. Li, L. Zhan, Y. Liu, C.Z. Huang, One-step synthesis of fluorescent hydroxyls-coated carbon dots with hydrothermal reaction and its application to optical sensing of metal ions, Sci China Chem, 54(2011) 1342-7.

[11] S. Liu, J. Tian, L. Wang, Y. Zhang, X. Qin, Y. Luo, et al., Hydrothermal Treatment of Grass: A Low-Cost, Green Route to Nitrogen-Doped, Carbon-Rich, Photoluminescent Polymer Nanodots as an Effective Fluorescent Sensing Platform for Label-Free Detection of Cu(II) Ions, Adv Mater, 24(2012) 2037-41.
[12] C.W. Lai, Y.H. Hsiao, Y.K. Peng, P.T. Chou, Facile synthesis of highly emissive carbon dots from pyrolysis of glycerol; gram scale production of carbon dots/mSiO(2) for cell imaging and drug release, J Mater Chem, 22(2012) 14403-9.
[13] X. Wang, K. Qu, B. Xu, J. Ren, X. Qu, Microwave assisted one-step green synthesis of cell-permeable multicolor photoluminescent carbon dots without surface passivation reagents, Journal of Materials Chemistry, 21(2011) 2445-50.
[14] H. Peng, J. Travas-Sejdic, Simple Aqueous Solution Route to Luminescent Carbogenic Dots from Carbohydrates, Chem Mater, 21(2009) 5563-5.
[15] Z. Liu, Y. Jiao, Y. Wang, C. Zhou, Z. Zhang, Polysaccharides-based nanoparticles as drug delivery systems, Adv Drug Delivery Rev, 60(2008) 1650-62.
[16] D.M.W. Anderson, W.G. Brydon, M.A. Eastwood, D.M. Sedgwick, Dietary effects of sodium alginate in humans, Food Addit Contam, 8(1991) 237-48.
[17] S.F. Chin, S.C. Pang, S.H. Tay, Size controlled synthesis of starch nanoparticles by a simple nanoprecipitation method, Carbohydrate Polymers, 86(2011) 1817-9.
[18] F. Grieser, M. Ashokkumar, J.Z. Sostaric, Sonochemistry and sonoluminescence in colloidal systems, Nato Adv Sci I C-Mat, 524(1999) 345-62.
[19] E.S.K. Tang, M. Huang, L.Y. Lim, Ultrasonication of chitosan and chitosan nanoparticles, Int J Pharm, 265(2003) 103-14.
[20] X. Sun, Y. Li, Colloidal Carbon Spheres and Their Core/Shell Structures with Noble-Metal Nanoparticles, Angew Chem Int Ed, 43(2004) 597-601.
[21] J. Wei, J. Qiu, Unveil the Fluorescence of Carbon Quantum Dots, Adv Eng Mater, (2014) n/a-n/a.
[22] F. Du, F. Zeng, Y. Ming, S. Wu, Carbon dots-based fluorescent probes for sensitive and selective detection of iodide, Microchimica Acta, 180(2013) 453-60.
[23] X. Zhai, P. Zhang, C. Liu, T. Bai, W. Li, L. Dai, et al., Highly luminescent carbon nanodots by microwave-assisted pyrolysis, Chem Commun, 48(2012) 7955-7.
[24] L. Tang, R. Ji, X. Cao, J. Lin, H. Jiang, X. Li, et al., Deep Ultraviolet Photoluminescence of Water-Soluble Self-Passivated Graphene Quantum Dots, ACS Nano, 6(2012) 5102-10.
[25] J. Zhou, Z. Sheng, H. Han, M. Zou, C. Li, Facile synthesis of fluorescent carbon dots using watermelon peel as a carbon source, Materials Letters, 66(2012) 222-4.
[26] C. Hu, C. Yu, M. Li, X. Wang, J. Yang, Z. Zhao, et al., Chemically Tailoring Coal to Fluorescent Carbon Dots with Tuned Size and Their Capacity for Cu(II) Detection, Small, (2014) n/a-n/a.
[27] D. Leal, B. Matsuhiro, M. Rossi, F. Caruso, FT-IR spectra of alginic acid block fractions in three species of brown seaweeds, Carbohydr Res, 343(2008) 308-16.
[28] X. Wang, L. Cao, F. Lu, M.J. Meziani, H. Li, G. Qi, et al., Photoinduced electron transfers with carbon dots, Chem Commun, (2009) 3774-6.
[29] Y.-L. Zhang, L. Wang, H.-C. Zhang, Y. Liu, H.-Y. Wang, Z.-H. Kang, et al., Graphitic carbon quantum dots as a fluorescent sensing platform for highly efficient detection of Fe3+ ions, RSC Advances, 3(2013) 3733-8.
[30] K. Qu, J. Wang, J. Ren, X. Qu, Carbon Dots Prepared by Hydrothermal Treatment of Dopamine as an Effective Fluorescent Sensing Platform for the Label-Free Detection of Iron(III) Ions and Dopamine, Chemistry – A European Journal, 19(2013) 7243-9.
[31] S.J.S. Flora, V. Pachauri, Chelation in Metal Intoxication, International Journal of Environmental Research and Public Health, 7(2010) 2745-88.

[32] G. Papanikolaou, K. Pantopoulos, Iron metabolism and toxicity, Toxicol Appl Pharmacol, 202(2005) 199-211.
[33] Council Directive 98/83/EC on the quality of water intended for human consumption, Official Journal of the European Communities1998.

469 Table 1. The relative errors caused by interfering species during the determination of Fe(III)

470 ions with 1:1 ratio and both the final concentrations were fixed at 1.56 mM respectively.

Interfering ions	***Relative error (%)***
Na(I)	0.70
K(I)	1.36
Mg(II)	0.54
Ca(II)	2.18
Ba(II)	2.59
Cr(III)	12.0
Mn(II)	3.04
Co(II)	5.94
Ni(II)	4.05
Cu(II)	4.08
Ag(I)	6.73
Zn(II)	1.12
Hg(II)	1.20
Sn(II)	55.7
Pb(II)	3.53

471

472

472 Table 2. Recovery of Fe(III) ions in spiked tap water samples

Fe(III) ions spiked (μM)	*Fe(III) ions recorded (μM)*	*Recovery rate (%)*	*RSD value (%)*
6.45	6.22	96.53	1.78
16.10	15.98	99.25	1.88
24.14	23.96	99.27	0.46
32.21	30.50	94.71	0.83

473

474

475

476

476 **Biographies**

477 **Jessica Fung Yee Fong** is currently doing her Ph.D. at the Faculty of Engineering,
478 Computing and Science, Swinburne University of Technology Sarawak Campus, Malaysia.
479 She received her B.Biotech. (Hons.) at University of Queensland, Australia in 2010. Her
480 research interest is the development of carbon nanoparticles for sensor applications.

481 **Suk Fun Chin** is an Associate Professor in material chemistry at the Faculty of Resource
482 Science and Technology, Universiti Malaysia Sarawak. She received her Ph.D. degree from
483 the School of Biomedical, Biomolecular and Chemical Sciences, University of Western
484 Australia, Australia in 2009. Her current research interests focus on synthesis and
485 characterisation of nanostructured materials.

486 **Sing Muk Ng** is the Associate Director (Science) of Swinburne Sarawak Research Centre of
487 Sustainable Technologies and senior lecturer at the Faculty of Engineering, Computing and
488 Science, Swinburne University of Technology Sarawak Campus, Malaysia. He obtained his
489 Ph.D. degree in analytical chemistry from the University of Manchester, United Kingdom.
490 His current research interests include development of bio/chemical optical sensors and light
491 instrumentations for chemical sensing applications.

492

Highlights

- Alginate nanoparticles was synthesised via ultrasonic-assisted nanoprecipitation
- Alginate nanoparticles was converted to carbon nanoparticles via acid dehydration
- Carbon nanoparticles formed were fluorescent
- Carbon nanoparticles were used as optical sensing probe for ferric ions

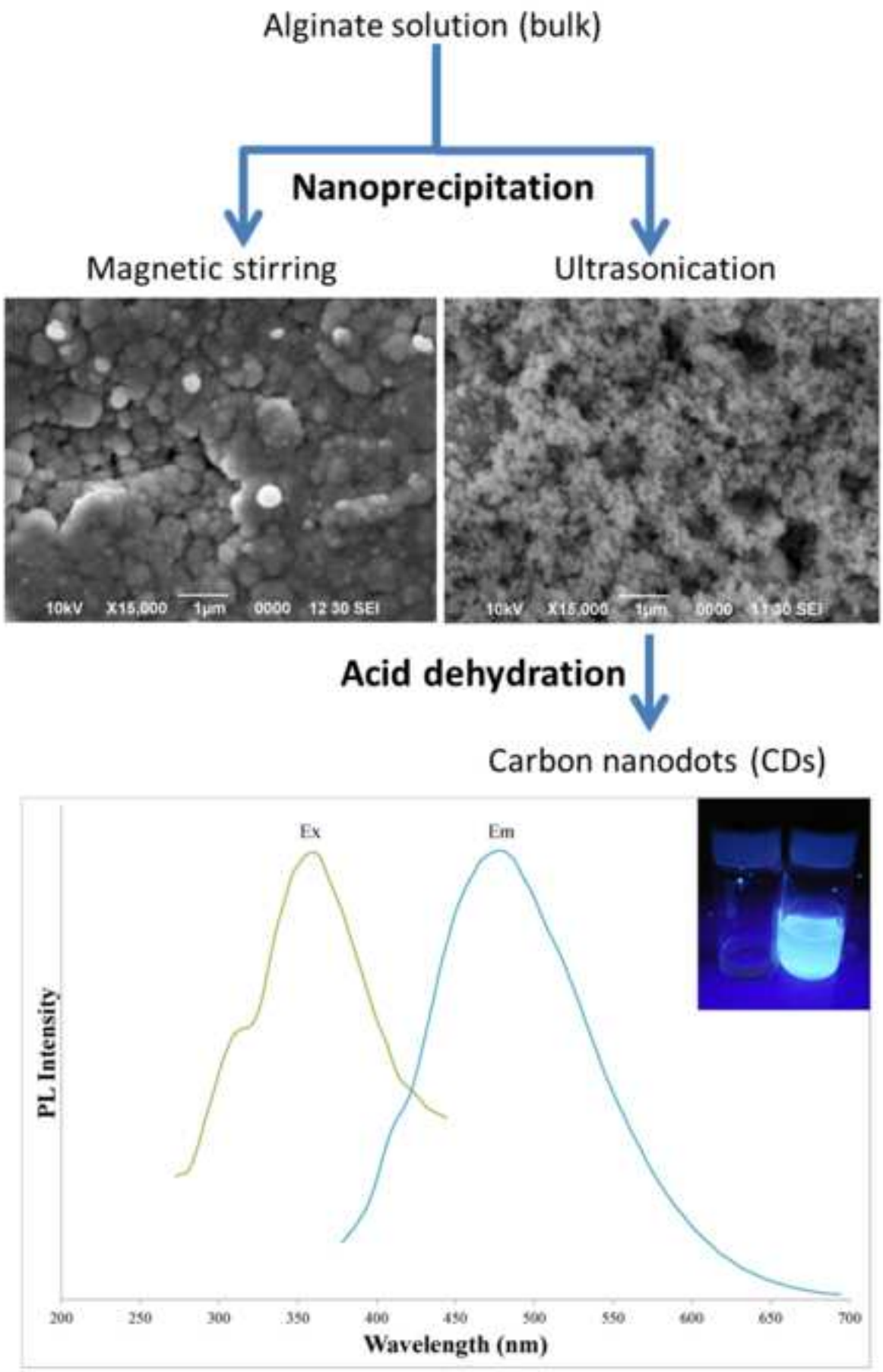

Figure 1

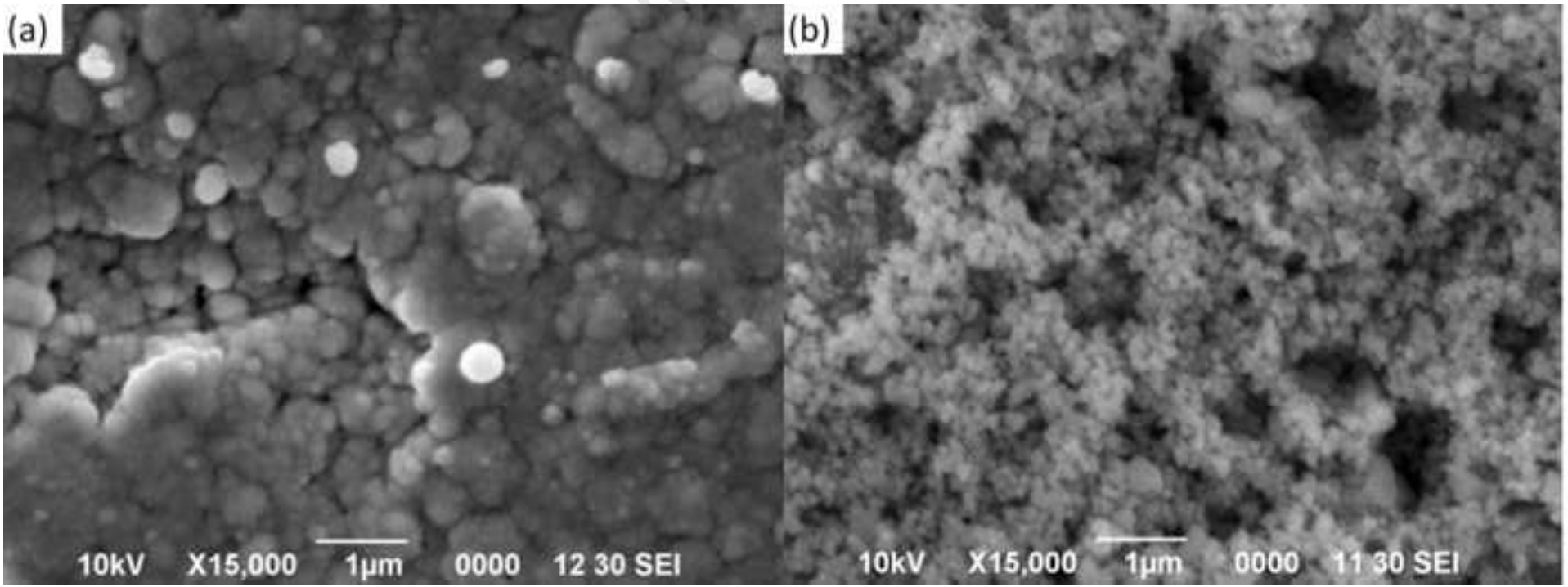

Figure 2

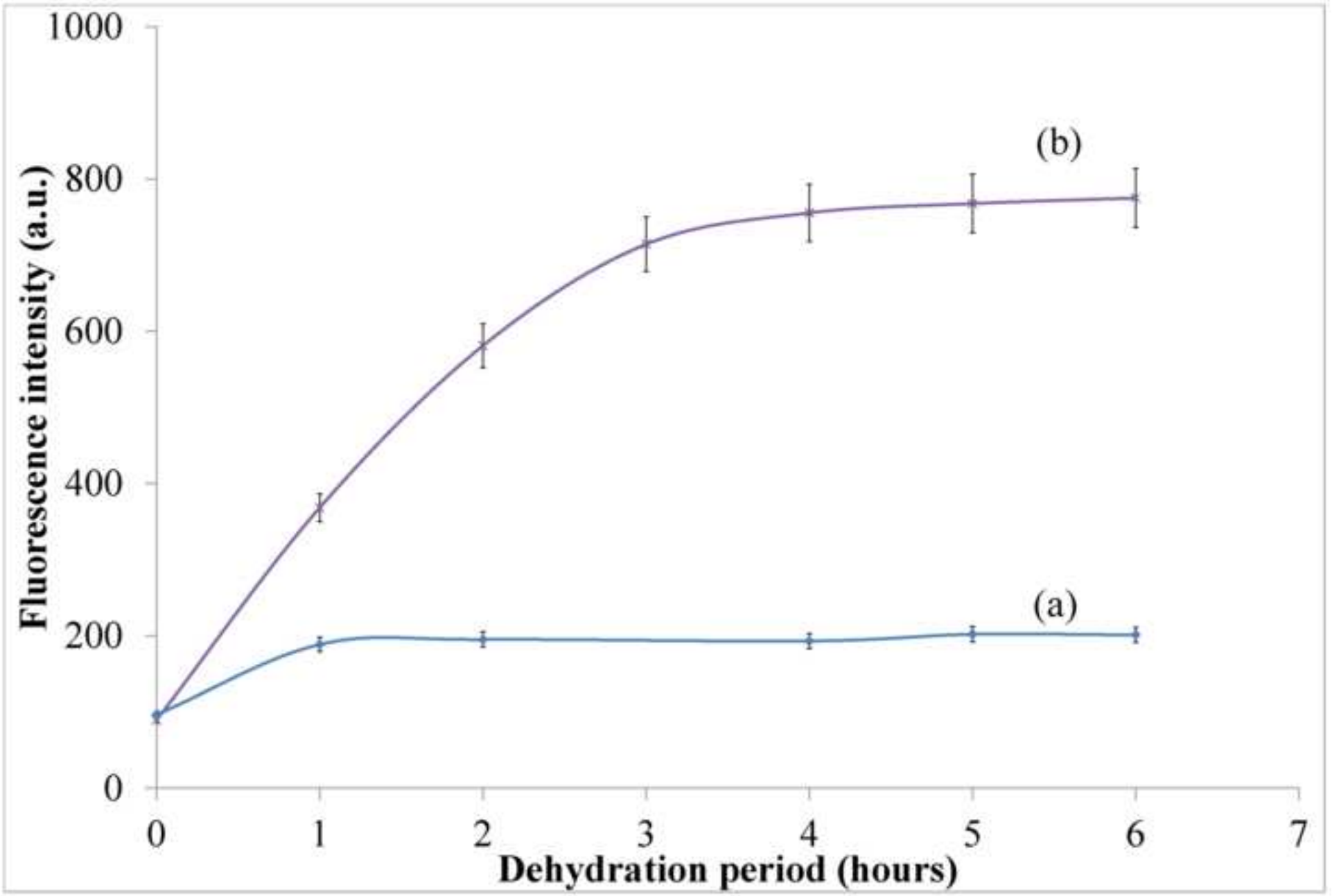
1000
800
600
400
200
0
Fluorescence intensity (a.u.)
(b)
(a)
0
1
2
3
4
5
6
7
Dehydration period (hours)

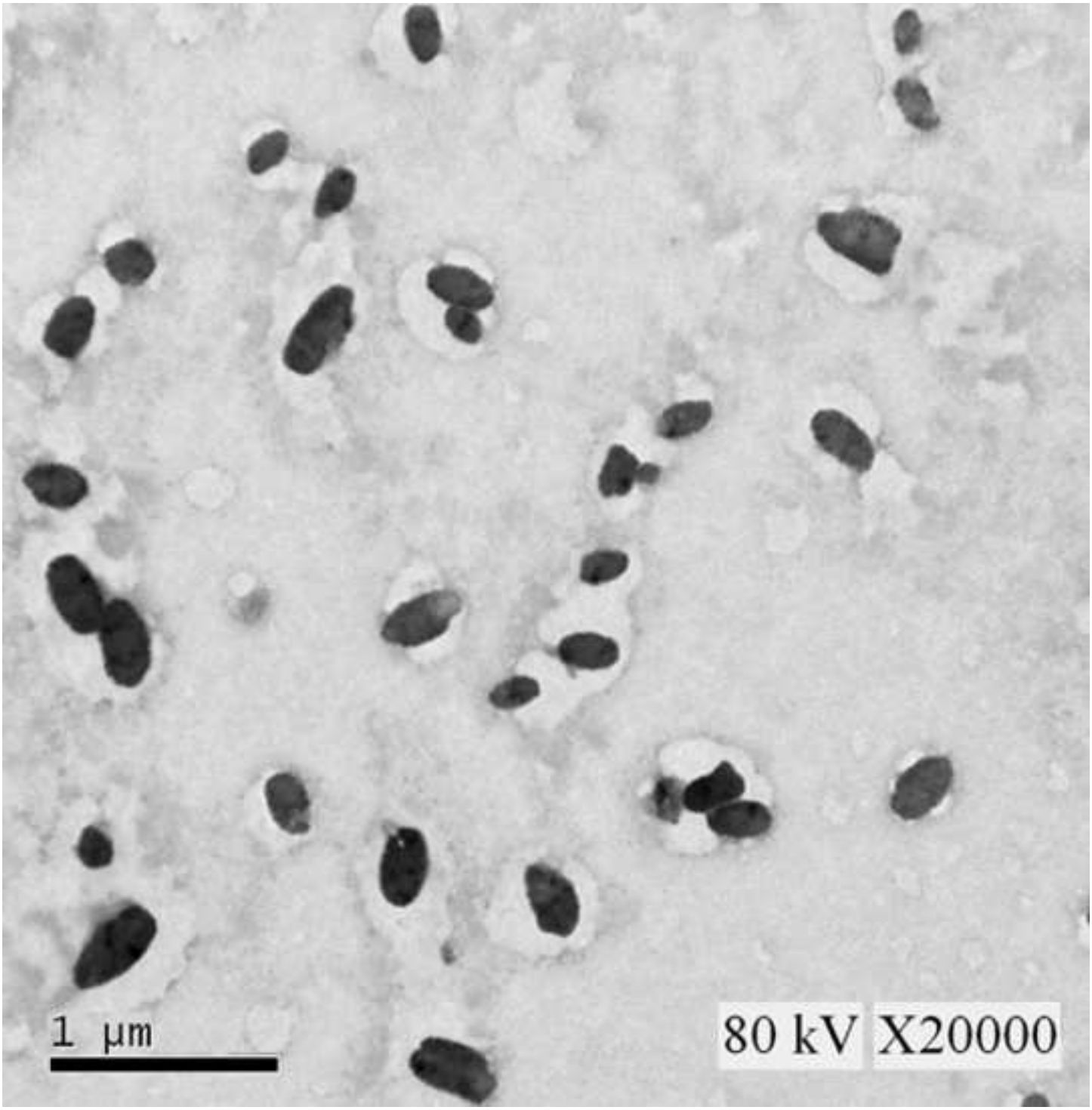

Figure 4a

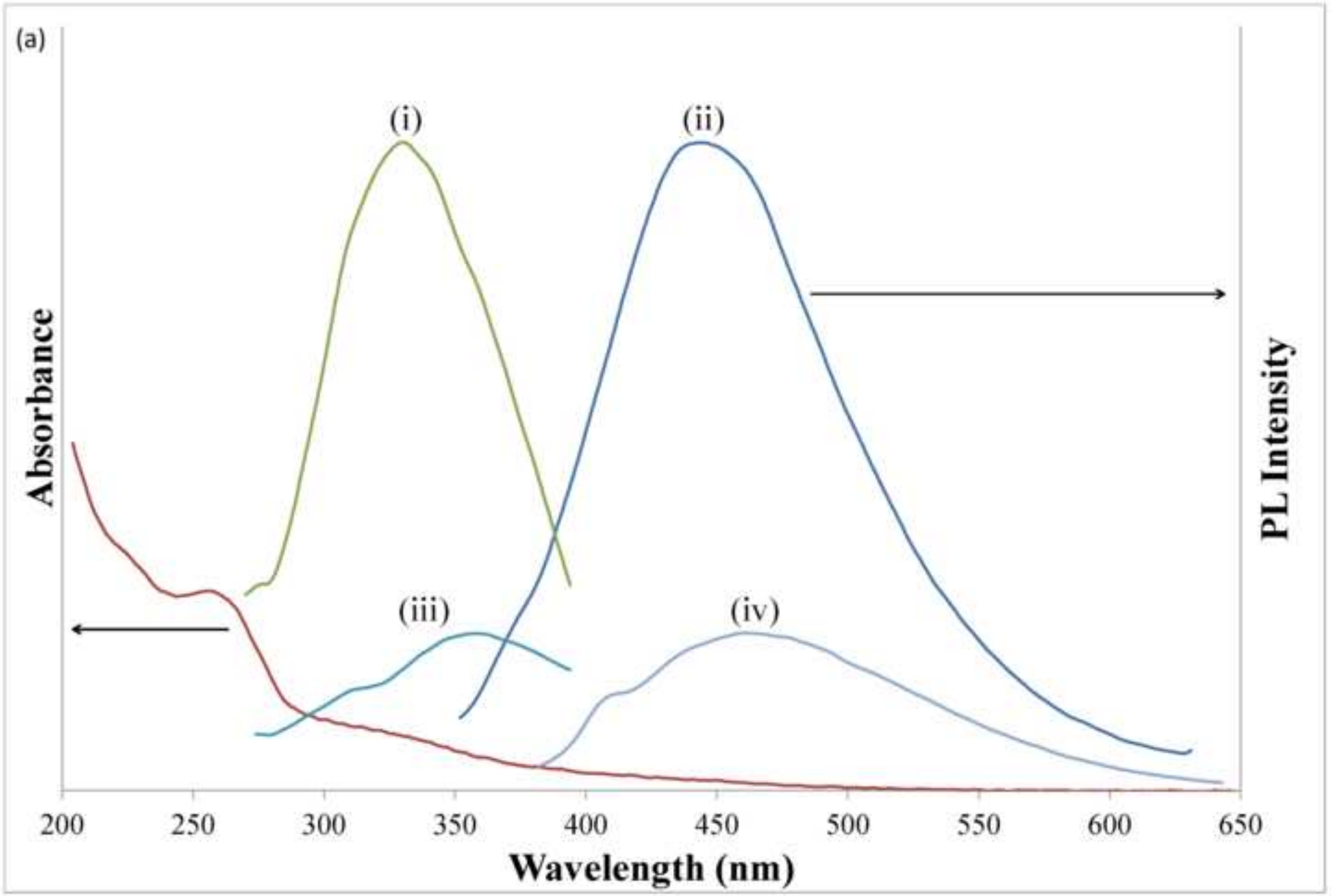
(a)
(i)
(ii)
(iii)
(iv)
Absorbance
PL Intensity
200
250
300
350
400
450
500
550
600
650
Wavelength (nm)

Figure 4b

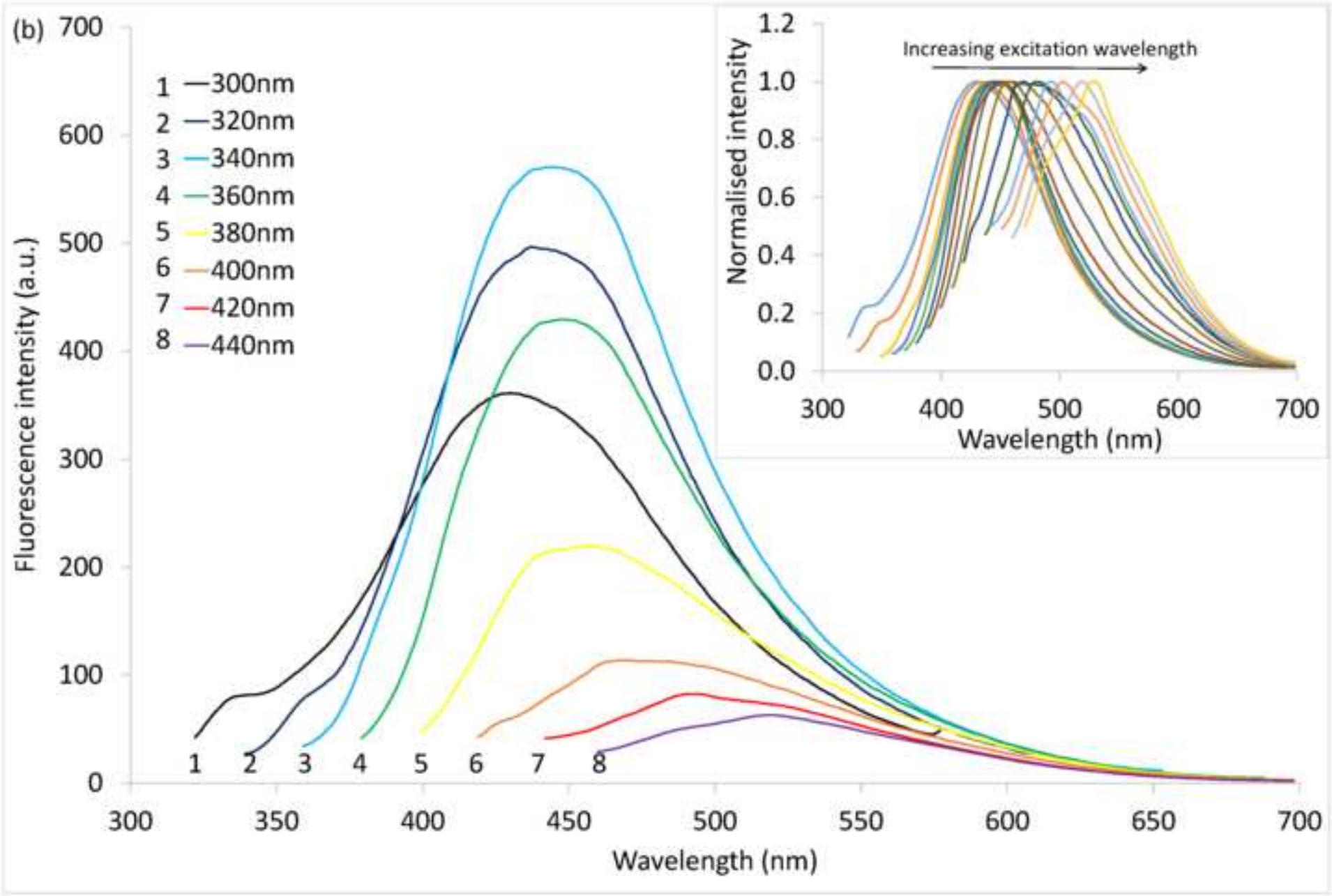
(b)
Fluorescence intensity (a.u.)
Wavelength (nm)
1 —300nm
2 —320nm
3 —340nm
4 —360nm
5 —380nm
6 —400nm
7 —420nm
8 —440nm
Normalised intensity
Increasing excitation wavelength
Wavelength (nm)

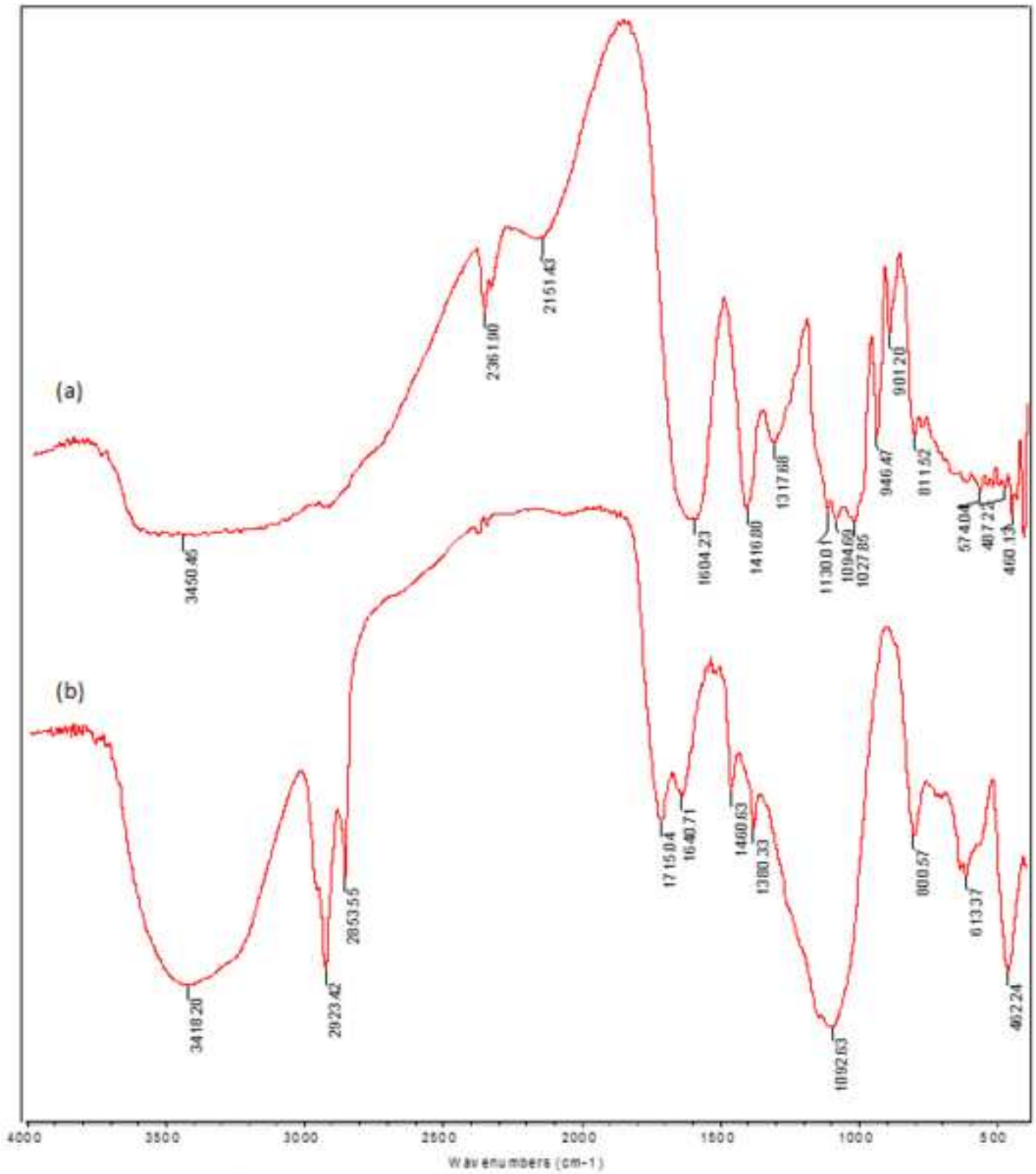

Figure 6

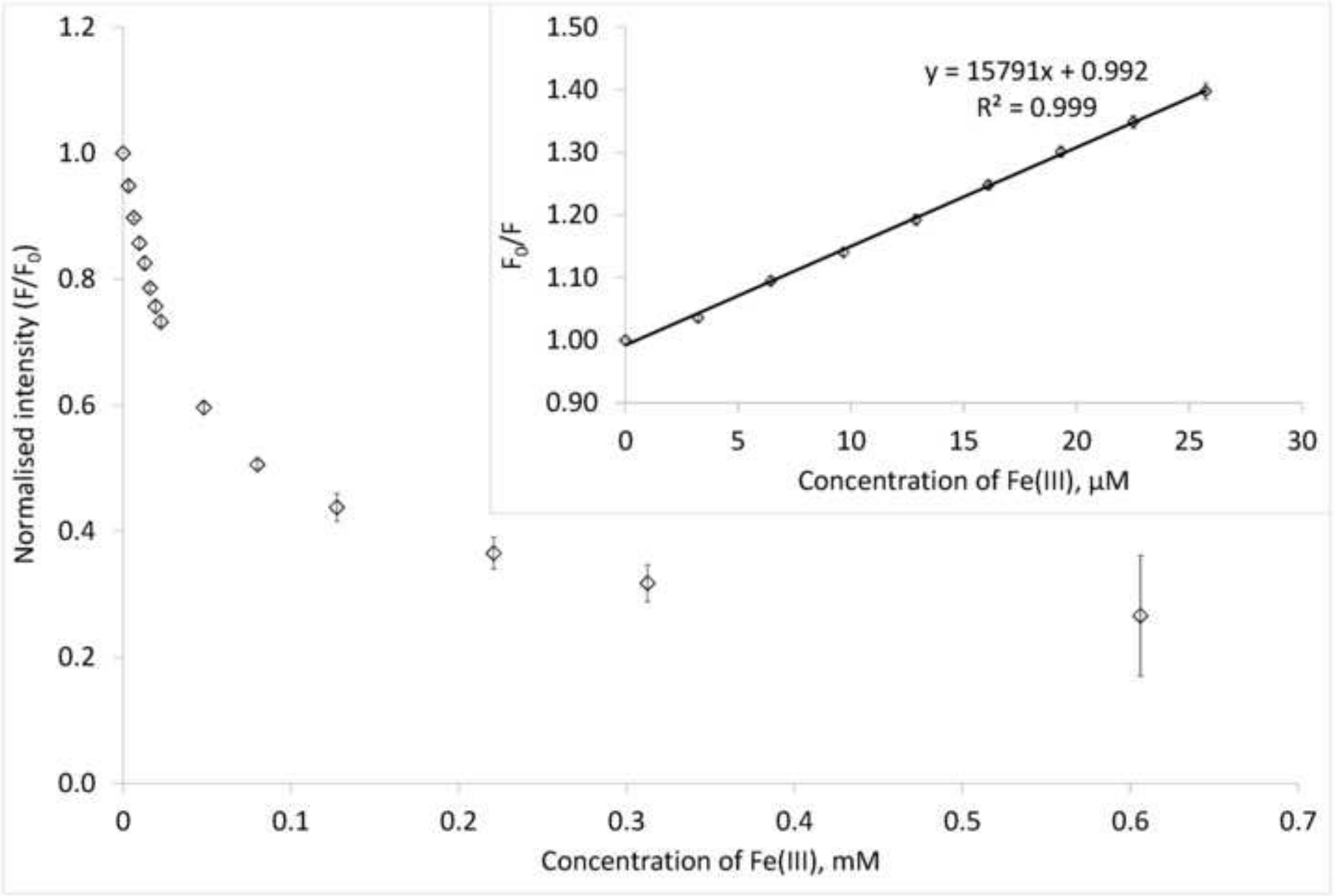
Normalised intensity (F/F0)
1.2
1.0
0.8
0.6
0.4
0.2
0.0
0
0.1
0.2
0.3
0.4
0.5
0.6
0.7
Concentration of Fe(III), mM
F0/F
1.50
1.40
1.30
1.20
1.10
1.00
0.90
y = 15791x + 0.992
R² = 0.999
0
5
10
15
20
25
30
Concentration of Fe(III), µM

Figure 7

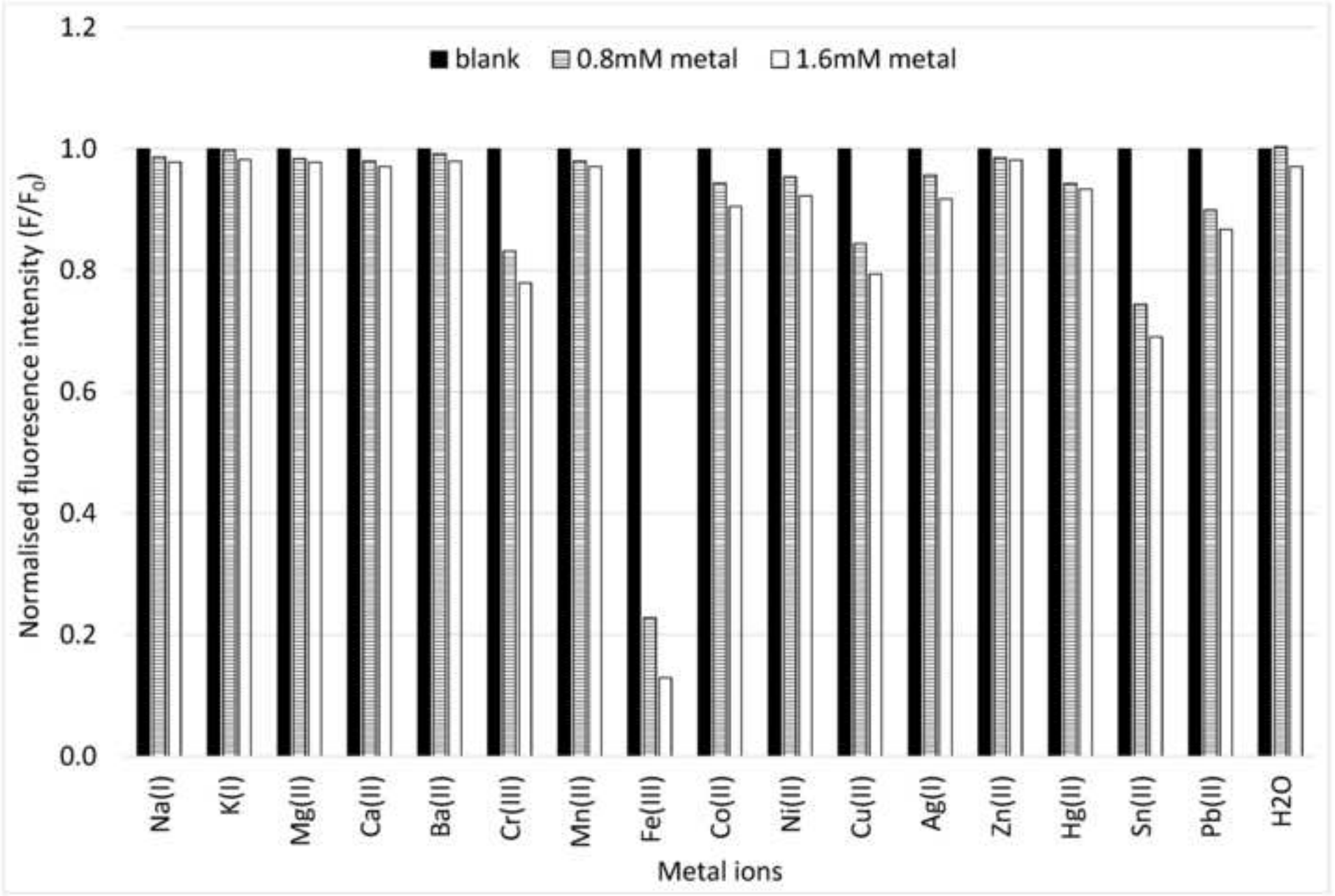
blank
0.8mM metal
1.6mM metal
Normalised fluoresence intensity (F/F0)
1.2
1.0
0.8
0.6
0.4
0.2
0.0
Na(I)
K(I)
Mg(II)
Ca(II)
Ba(II)
Cr(III)
Mn(II)
Fe(III)
Co(II)
Ni(II)
Cu(II)
Ag(I)
Zn(II)
Hg(II)
Sn(II)
Pb(II)
H2O
Metal ions

Figure captions:

Figure 1. SEM images that depict the morphology difference between the alginate nanoparticles obtained by nano-precipitation using (a) magnetic stirring and (b) ultrasonication approaches.

Figure 2. An observation in changes of fluorescence intensity of CNPs as the dehydration period increases when the carbonisation was performed at (a) room temperature and (b) 120°C.

Figure 3. TEM image of the CNPs produced from the thermal acid carbonisation of alginate nanoparticles .

Figure 4. (a) The absorbance of the CNPs (directed with arrow) and the photoluminescence profile of the CNPs, where (i) is the fluorescence excitation spectrum obtained at 440 nm and (ii) is the emission band when excited at 340 nm. Comparison spectrums were taken from CNPs obtained from alginate nanoparticles pre-processed with magnetic stirring as shown by (iii) and (iv) respectively. (b) Fluorescence emission spectrum of CNPs at different excitation wavelengths from 300 nm to 440 nm.

Figure 5. FTIR spectrum of (a) the starting material, alginate and (b) the product, CNPs.

Figure 6. Fluorescence spectrums showing the quenching effect upon consecutive addition of Fe(III) ions into the CNPs sensing solution. The sublet plot shows fluorescent detection of Fe(III) ions being fitted into Stern-Volmer plot.

Figure 7. Fluorescence response of the CNPs towards a series of possible interfering ions upon excitation of 340 nm. *The sequence of interferents is arranged accordingly to their group in periodic table.